Observation of 3–6-Day Meridional Wind Oscillations over the Tropical Pacific, 1973–1992: Horizontal Structure and Propagation

TIMOTHY J. DUNKERTON AND MARK P. BALDWIN

Northwest Research Associates, Bellevue, Washington

(Manuscript received 10 February 1994, in final form 19 September 1994)

ABSTRACT

Twenty years of rawinsonde data (1973–1992) were examined in conjunction with European Centre for Medium-Range Weather Forecasts (ECMWF) analyses and outgoing longwave radiation (OLR) in 1980–1989 to determine the horizontal structure, propagation, and convective coupling of 3–6-day meridional wind oscillations over the tropical Pacific. Wave properties from ECMWF data, determined by lag correlation with respect to rawinsonde or ECMWF principal components, were consistent with what could be determined from the sparse rawinsonde network alone. Gridded analyses allowed a clearer distinction between equatorially trapped Rossby–gravity waves (RGW) and off-equatorial "tropical-depression" (TD) disturbances, so that the contrasting properties of these waves, including their seasonal and interannual variation, could be studied in better detail. Significant correlations with OLR were found, increasing in magnitude from eastern to western Pacific.

The apparent group propagation of disturbances was equatorward in the western Pacific, eastward across the central and eastern Pacific, and upward–downward out of the 150–300-mb layer. Vertical propagation was evident primarily at higher frequencies, implying that only a fraction of the kinetic energy associated with Rossby–gravity waves in the upper troposphere was involved either in convective coupling to the lower troposphere or vertical momentum transport to the lower stratosphere. It is suggested that in addition to convective and lateral forcings, Rossby–gravity waves are sometimes excited by energetic TD disturbances in the western Pacific.

1. Introduction

The tropical troposphere contains a complex assortment of meteorological phenomena ranging in horizontal scale from cumulonimbus clouds and mesoscale convective systems, to intraseasonal oscillations and planetary-scale circulations. Of the various phenomena, synoptic-scale disturbances (1500–10 000 km) arguably are the most important because they organize tropical convection and precipitation at shorter scales and comprise the inner scale of planetary circulations. Along the equator, superclusters lie within intraseasonal oscillations (Nakazawa 1988; Mapes and Houze 1993). Tropical convergence zones are stormtracks tracing the locus of deep convection within propagating synoptic-scale waves (Hack et al. 1989; Hess et al. 1993).

Until the early 1980s, knowledge of synoptic-scale phenomena was based on meteorological observations from isolated upper-air stations and a few intensive observing campaigns. Although the major disturbance characteristics were well described in certain regions (Wallace 1971; Yanai 1975), a global perspective was impossible. Where available, station data were sometimes ambiguous and confusing.

Global analyses—based not only on rawinsonde observations but also satellite-derived temperatures and cloud winds—now reveal the complexity of tropical circulation in more detail. These data afford a better description of horizontal structure and propagation than possible with rawinsonde data alone (Zangvil and Yanai 1980, 1981; Yanai and Lu 1983; Nitta et al. 1985; Nitta and Takayabu 1985; Liebmann and Hendon 1990). In the central and western tropical Pacific, where many of the early rawinsonde studies were concentrated, synoptic-scale waves in the lower troposphere evidently may be classified as "equatorial waves" situated symmetrically or antisymmetrically about the equator (in accord with linear wave theory) and off-equatorial tropical depression (TD) waves or vortical structures akin to the familiar "easterly waves" of early literature (Takayabu and Nitta 1993). Both disturbances regulate, and are in turn influenced by, deep tropical convection at least part of the time. In the central Pacific, equatorial Rossby–gravity waves maximize in northern autumn (Hendon and Liebmann 1991), while TD disturbances prevail farther west, maximizing in northern summer (Takayabu and Nitta 1993). The annual variations are consistent with changes in underlying sea surface temperature (SST) if the waves are coupled to convection and derive en-

Corresponding author address: Dr. Timothy J. Dunkerton, Northwest Research Associates, P.O. Box 3027, Bellevue, WA 98009-3027.

ergy from latent heat release. The importance of convection is suggested by cross-spectrum analysis with cloud observations, analysis of the energy budget and (for Rossby–gravity waves) by inserting a moist equivalent depth in the RGW dispersion relation (Lau and Lau 1990, 1992; Hendon and Liebmann 1991; Takayabu and Nitta 1993). Interannual variations of wave activity are likewise consistent with SST variations where convective coupling occurs.

In addition to convective Rossby–gravity waves and TD disturbances originating in the lower troposphere are shear-modified Rossby–gravity waves attaining largest amplitude in the upper troposphere over the eastern equatorial Pacific (Randel 1992). These waves are not significantly coupled to convection but apparently depend on lateral excitation from baroclinic systems in the midlatitude Southern Hemisphere (see also Zangvil and Yanai 1980, 1981; Magaña and Yanai 1994).

At present, several questions remain unanswered. For example, 1) the relative importance of convective and laterally forced waves in the troposphere and lower stratosphere is unknown; 2) the relation, if any, of upper tropospheric waves to the lower tropical troposphere is unclear; 3) in the lower troposphere, it is uncertain whether equatorial waves and TD disturbances are entirely distinct or evolve continuously from one type to the other as the background environment changes (e.g., from central to western Pacific); 4) seasonal and interannual variations of SST alter the geographical distribution of wave activity, but these variations have not been extensively studied, particularly in data-sparse regions (e.g., eastern Pacific); and 5) when using winds derived entirely from analyses, there is naturally some concern whether observed phenomena are genuine or a model artifact. With the exception of Randel (1992), none of the recent papers used rawinsonde data for validation.[1]

To address these questions, we are investigating available rawinsonde data from the tropical troposphere and lower stratosphere beginning in 1973, together with gridded analyses beginning in 1980. Some preliminary results from rawinsonde data were reported in Dunkerton (1991) for the lower stratosphere throughout the Tropics and in Dunkerton (1993, hereafter D93) for the troposphere and lower stratosphere over the western, central, and southeastern equatorial Pacific. Several results of D93 were consistent with early rawinsonde studies (Yanai and Maruyama 1966; Yanai et al. 1968; Yanai and Hayashi 1969; Nitta 1970) and more recent investigations with analysis data. Four types of meridional wind oscillations were revealed: 1) a modified Rossby–gravity wave maximizing in upper troposphere (period 5–6 days, zonal wavenumber 4–6), not significantly coupled to the lower troposphere or lower stratosphere; 2) a convectively coupled Rossby–gravity wave maximizing in the central Pacific, lower troposphere (period 4–5 days), but with radiating tail extending vertically into the upper troposphere and lower stratosphere; 3) waves of short zonal scale in the lower troposphere west of the date line, occupying a broad band of frequencies; and 4) stratospheric Rossby–gravity waves (period 3–4 days, zonal wavenumber 3–4). Dominant wave periods and zonal wavelengths were inferred from cross-spectrum analysis of meridional wind. Wavelengths could be estimated only at stations west of the date line near the same latitude (7°–10° N). Cross-equatorial symmetry could be inferred only near the date line.

Seasonal and interannual variations of wave activity were also discussed by D93 and appear consistent with other studies (e.g., Chang and Miller 1977; Yanai and Lu 1983) concerning the effect of El Niño/Southern Oscillation (ENSO) on upper tropospheric waves and with Maruyama (1991) on the role of the stratospheric quasi-biennial oscillation (QBO).

As a continuation of D93, we now discuss the horizontal structure and propagation associated with 3–6-day meridional wind oscillations using gridded analyses in conjunction with rawinsonde data. Similar vertical structures are obtained from both datasets, and significant temporal correlations are found, validating the features observed in gridded data. Section 2 discusses the data analysis and methods, section 3 identifies the dominant vertical and horizontal structures, and section 4 discusses the horizontal wavelength, phase propagation, and apparent group propagation of the various disturbances throughout the Pacific sector. Seasonal and interannual variations are discussed briefly in section 5.

2. Data analysis

Rawinsonde data were analyzed at ten stations in the western, central, and southeastern equatorial Pacific (see Table 1 of D93) from a subset of 40+ stations within 10° of the equator identified by Dunkerton (1991) as having copious data in the troposphere and lower stratosphere since 1973. Measurements were typically made once or twice per day (e.g., near 0000 or 1200 UTC) and occasionally at other times, so that binned, interpolated soundings were stored four times daily. Rawinsonde time series extended from 1 January 1973 through 18 April 1992. The quality control, interpolation, and spectral analysis were described in D93. Dominant oscillations were identified from coherence of meridional wind at the same station or between adjacent stations. Examples of coherence spectra and zonal wavelengths in D93 agreed with earlier results based on one or two intensive observing periods (e.g., Yanai et al. 1968).

[1] Analyzed winds in the lower troposphere correlate well with cloud proxy data in regions of convective coupling (Hendon and Liebmann 1991; Takayabu and Nitta 1993).

Rotated principal component analysis was performed in D93 by constructing covariance or correlation matrices within a few "synoptic networks" consisting of stations aligned parallel to the equator in west-central Pacific (from Kota Kinabalu to Tarawa) or stations near the date line on opposite sides of the equator (Majuro, Tarawa, and Funafuti). Cross-spectrum analysis of principal components revealed coherent, westward propagating patterns in agreement with results obtained directly from individual stations. Time histories of their quadrature spectra described seasonal and interannual variations of wave activity.

In this paper, we supplement rawinsonde data with 2.5° × 2.5° gridded analyses from the European Centre for Medium-Range Weather Forecasts (ECMWF) and outgoing longwave radiation (OLR) datasets. Initialized ECMWF analyses (twice daily) and OLR data (once daily) were obtained for the time period 1 January 1980 to 31 December 1989. There were at most 7306 points of overlap between ECMWF and rawinsonde time series. EOFs obtained from rawinsondes in 1980–1989 were indistinguishable from those obtained from the full record (1973–1992), so the latter were used here.

Our analysis of correlations between rawinsonde and gridded analyses began with individual station time series of meridional wind and principal components derived from the synoptic networks of D93. Point correlations were similar to those determined by Randel (1992). These lay in the range 0.60–0.90 and were highly significant but uninteresting; the spatial patterns were simply bull's eyes centered near the station location with small radius (a few degrees). This comparison established the accuracy of ECMWF anomaly fields, but there are evidently many phenomena passing over individual stations so that the coherence length is quite small when all scales of motion are included. This is a major limitation of one-point correlation analysis in the tropical troposphere.

Correlations between rawinsonde principal components of D93 and ECMWF data were more illuminating, giving significant patterns extending over many days time lag, several tens of degrees longitude, and most latitudes of the tropical belt. Meaningful results could be obtained using extended EOFs from individual stations, even at isolated locations. For this purpose, correlation matrices were constructed at each station on a two-dimensional grid having the vertical coordinate as one direction (at standard pressure levels 850, 700, 500, 400, 300, 250, 200, 150, 100, 70, 50, and 30 mb) and time lag as the other. Meridional wind v', zonal wind u', and temperature T' were combined into a single matrix; similar results were obtained from meridional wind alone. This method is a further extension (to many time lags) of "extended, multivariate, rotated principal component analysis" in which spatially gridded data are arrayed at a few time lags (Lau and Lau 1990) or, alternatively, an extension of "singular spectrum analysis" of time series (Ghil and Mo 1991) to include a spatial coordinate, several variables, and varimax rotation as well as time lag. As in SSA, the window length is arbitrary; optimum results are obtained if anywhere from one-half to a full cycle of the dominant oscillation fit into the window. (Longer windows produce degenerate EOFs, while shorter windows misrepresent oscillations as a trend.) An increment of one-half day was sufficient for time lags, with maximum lag ±3 days. For single-station extended EOFs, the resulting correlation matrix had dimension (13 lags) × (3 variables) × (12 levels) = 468. Dominant oscillations appeared as a pair of EOFs approximately in quadrature, with coherent principal components. Varimax rotation was used to optimize coherence between rotated PCs, including up to 24 EOFs in the rotation.

As in D93, data were prefiltered to exclude low frequencies. Examples of frequency response using combinations of triangle filters (as in D93) are shown in Figs. 1a, b for highpass and bandpass, respectively. For most of the results shown in this paper, a single highpass filter was applied (−,24 in the notation of D93) with half-power response at about 12 days and nearly full response at higher frequencies. This gave an objective, though imperfect, definition of dominant EOFs. (Filtering did not predetermine the wave period, but more than one disturbance was sometimes found in the same EOF.) Once the dominant wave periods were objectively determined, principal component analysis was repeated with bandpass filters suited to each disturbance. This gave a more accurate definition of wave structure and amplitude variability.

Results did not greatly depend on the choice of filter as long as the lowest frequencies (e.g., Hadley circulation) were excluded, as in D93. Care must be taken when using SSA on prefiltered data since, as shown by Ghil and Mo (1991) even red noise can produce an oscillation. This did not affect any of the structures reported here.

Principal component analysis also used ECMWF data as input. This was done in one of two ways, vertically or horizontally. 1) Meridional wind was arrayed in the longitude–height plane on 24 × 7 grids of length 60° or 120° at standard levels (1000, 850, 700, 500, 300, 200, and 100 mb). The grids were placed at any of 36 starting longitudes (10° apart) along 5° latitude circles (10°S, 5°S, equator, 5°N, 10°N). 2) Meridional wind, zonal wind, and OLR were arrayed in the longitude–latitude plane on 8 × 9 grids of various sizes (40° × 20°, 40° × 40°, and 60° × 60°) at standard pressure levels, starting at any of 36 longitudes as in 1). To check that latitudinal structures were not influenced by sampling, the grids were centered at various latitudes—confirming that rotated EOFs are domain-independent. Results obtained from 2) provided many valuable insights on the dominant patterns of synoptic variability in the tropical troposphere, as well as some useful information on midlatitude baroclinic systems

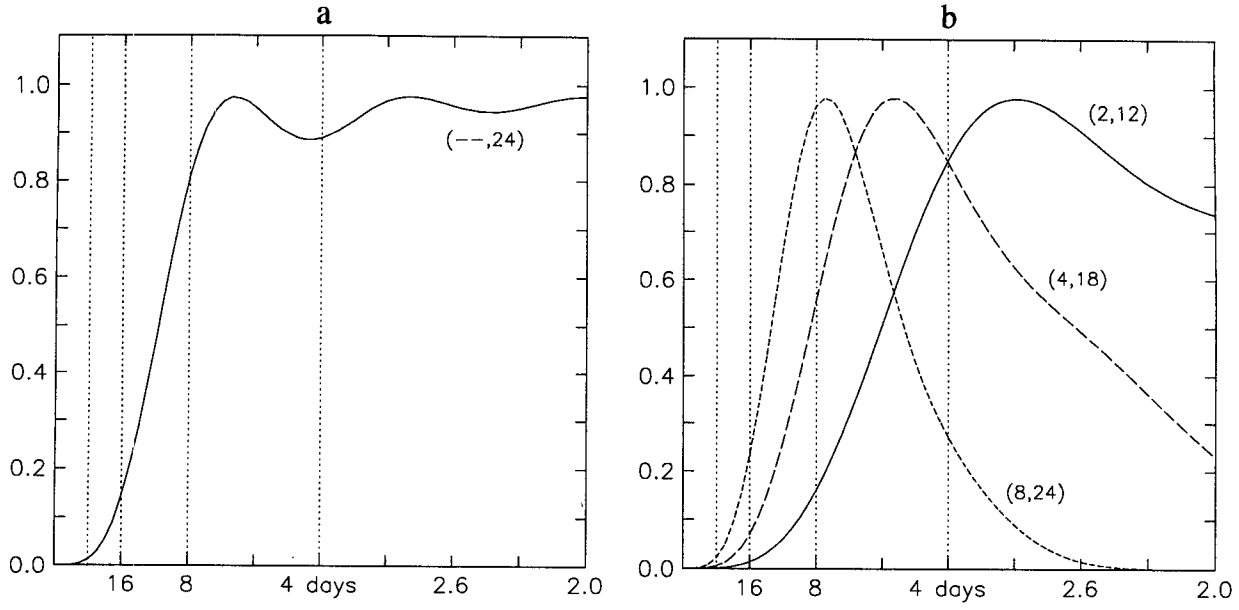

FIG. 1. Response of highpass (a) and bandpass (b) filters used in this study.

penetrating the Tropics. Since it is too extensive to discuss here, this material is reserved for a subsequent manuscript. In this paper we present results obtained in the Pacific sector at 700 mb using 40° × 40° grids centered on the equator.

3. Vertical and horizontal structures

a. Rawinsonde observations

Extended EOFs of rawinsonde data (v', u', and T') were obtained at the ten stations listed in Table 1 of D93. Several of these were identical in their v' component to EOFs of v' alone. Various structures were obtained, including upper-tropospheric waves at 150–300 mb (type A of D93), lower-tropospheric waves (1000–500 mb) with tilted baroclinic structure aloft (type B), and stratospheric Rossby–gravity waves (70–30 mb). These disturbances were characterized by a large meridional wind component. The analysis also revealed Kelvin waves in the stratosphere (for the first time using EOFs) and other tropospheric disturbances involving zonal wind and temperature that may be related to intraseasonal oscillations and the seasonal cycle. Attention is restricted to meridional wind oscillations in the 3–6-day range, concentrating on the troposphere where horizontal structure and propagation could be determined using gridded analyses. Our colorless terminology (A, B) will be used again because, as shown in section 4, these vertical structures sometimes contained a mix of disturbance types.

Examples of type A are shown in Figs. 2a–c. This structure, with maximum v' at 150–300 mb, was found at each of the ten stations. It was the dominant meridional wind oscillation at central and eastern Pacific stations but of secondary importance in the far western Pacific. The phase relation of meridional (v') and zonal (u') wind (not shown) was as follows. At Atuona, in the southeastern equatorial Pacific, u' led v', consistent with a westward propagating Rossby–gravity wave south of the equator. At Tarawa, in the central equatorial Pacific, the meridional wind had a similar pattern, but u' was negligible. At Majuro, north of Tarawa, u' lagged v', although the two were not in perfect quadrature, displaying a positive correlation as in D93. Vertical structure evolved gradually toward the western stations so that phase tilts were replaced by an out of phase "first baroclinic mode" (e.g., Koror). All of these structures in central and western Pacific were virtually the same as lag-correlation patterns with respect to the principal components of *spatial* EOFs obtained in D93.

The second EOF pair of meridional wind (type B) displayed a characteristic westward (eastward) tilt with height in upper (lower) troposphere at central and eastern Pacific stations, as shown in Figs. 3a–c (Majuro) and Figs. 4a–c (Atuona). (Westward propagation is assumed in translating the phase delay into a vertical tilt.) The phase relation between zonal and meridional wind switched upon crossing the equator. Likewise, the meridional heat flux switched sign so that the product $f\overline{v'T'}$ (where f is the Coriolis parameter and the overbar denotes an average over time lags) was in both hemispheres positive near the tropopause and negative in the lower troposphere. These patterns were consistent with an equatorial wave radiating upward above 200 mb and downward below that level. It may be tempting to discard the B pattern as an artifact of EOF

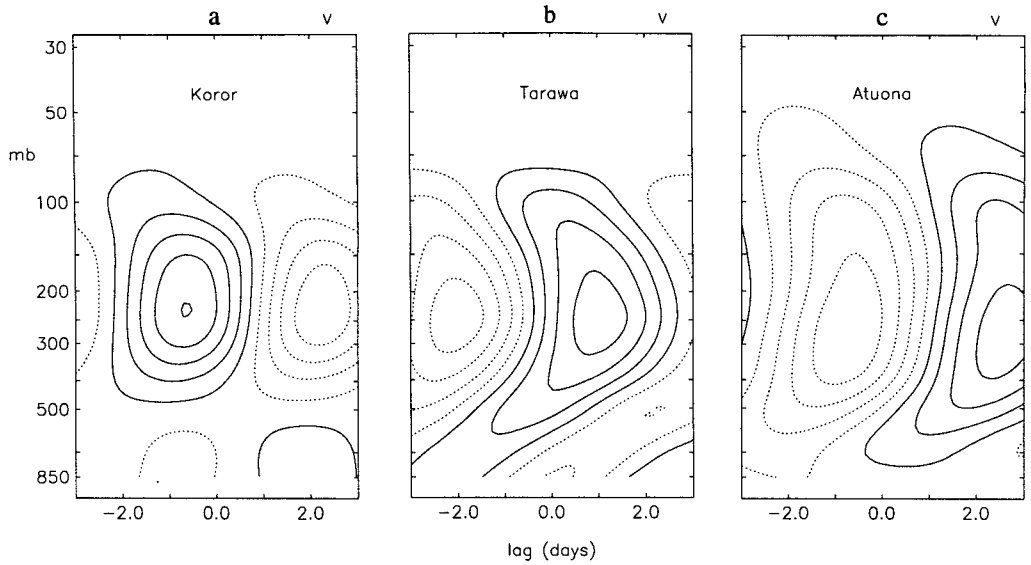

FIG. 2. Meridional wind structure associated with upper troposphere (type A) EOFs at various rawinsonde stations.

analysis given the orthogonality of unrotated EOFs. However, the pattern persists as many EOFs are rotated—reflecting a genuine correlation between the 100-mb level and the lower half of the troposphere (D93). Nearly identical results were obtained when the 150–300-mb layer was omitted.

At Tarawa the meridional wind structure of lower tropospheric waves was similar (Fig. 5c), but zonal wind and temperature (not shown) were negligible. At Truk (Fig. 5b) there was little vertical tilt. In the far western Pacific (Kota Kinabalu, Fig. 5a) there was modest westward tilt over a deep layer and a minor phase reversal in upper troposphere. In this region the order of A and B were reversed, suggesting a strong horizontally divergent component of rawinsonde velocities near the main Hadley cell.

The extended EOF technique gave meaningful results at isolated stations like Atuona (Figs. 2c, 4a–c). The B pattern at this location suggested an unusual, if not bizarre, coupling of lower troposphere and lower stratosphere (Fig. 4a). The interpretation of this pattern was elusive until recently (section 4).

b. *ECMWF observations*

Spatial EOFs of meridional wind were obtained from ECMWF data on various horizontal and vertical grids as described in section 2. Similar vertical structures (A, B) were found as in rawinsonde data; two examples are shown in Figs. 6a, b from the eastern Pacific. These were universal patterns—observed with significant coherence over the three tropical oceans—except for the western Pacific, where the dominant EOF pair displayed westward tilt with height as in Fig. 5a, and the second pair displayed a "first baroclinic mode" structure (not shown).

Figures 7a–c display the lag correlation of ECMWF v', u', and T' with respect to the principal component associated with Fig. 6a (type A). Correlations with respect to that of Fig. 6b are shown in Figs. 8a–c (type B). Zonal wind and temperature perturbations were approximately antisymmetric (not shown). Although the 100-mb data may not be completely reliable as the topmost level of initialized ECMWF data, correlation of meridional wind and temperature clearly suggested an upward flux of wave activity near the tropopause and a downward flux in lower troposphere, as in rawinsonde data. There was an apparent eastward and downward group propagation through the midtroposphere (Liebmann and Hendon 1990).

c. *Horizontal structures in ECMWF and OLR data*

Theoretical equatorial waves have a well-defined horizontal structure and cross-equatorial symmetry. As noted in the Introduction, it is primarily their horizontal structure and propagation that separates equatorially trapped waves from off-equatorial TD disturbances (Lau and Lau 1990, 1992; Takayabu and Nitta 1993) and from eastward traveling midlatitude baroclinic systems. Lau and Lau (1990) used principal component analysis in the horizontal plane to describe TD disturbances. Their method (involving 850-mb vorticity and a few time lags) was well suited for these disturbances since vorticity involves horizontal differentiation (emphasizing smaller scales) but apparently did not yield much useful information on equatorially trapped waves. Takayabu and Nitta (1993) separated the two waves using gridpoint correlation analysis of ECMWF data with respect to GMS equivalent blackbody temperatures (in western and central Pacific during northern summer).

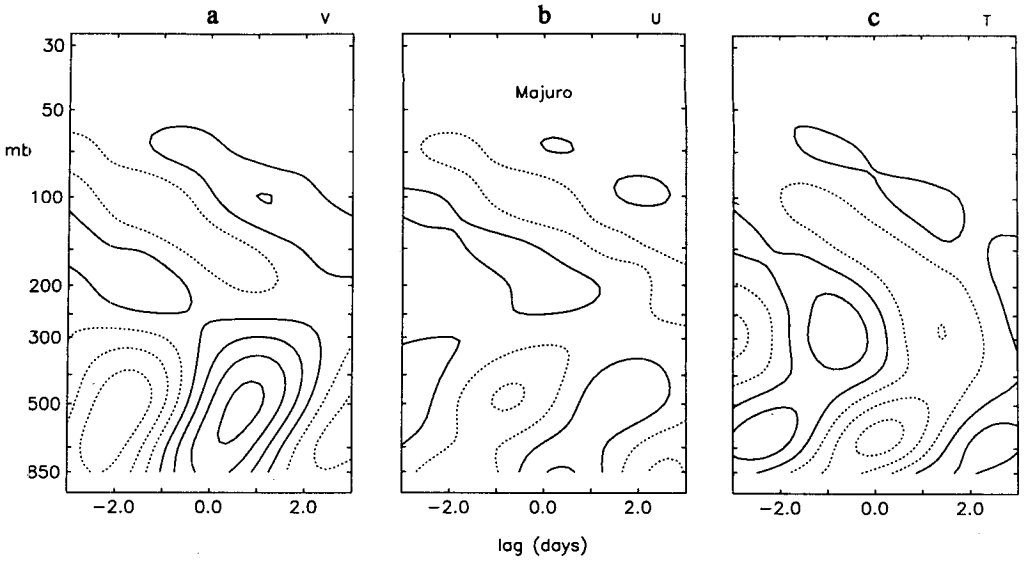

FIG. 3. Structure of lower troposphere (type B) EOF at Majuro. (a) Meridional wind; (b) zonal wind; and (c) temperature.

Wave structures are easily distinguished using the multivariate horizontal EOFs described in section 2 (u', v', and OLR). At 700 mb this technique, in contrast to that of Lau and Lau, tended to emphasize Rossby–gravity waves over TD disturbances, except in the western Pacific where TD disturbances attained large amplitude. Four examples of multivariate rotated EOFs are shown in Figs. 9a–d from western to eastern Pacific.

Major variations of wave structure were visible proceeding from western to eastern Pacific. In the west (Fig. 9a) the dominant pattern was centered north of the equator, with short zonal wavelength, consistent with a vortex train aligned towards the northwest (Lau and Lau 1990). Convection, indicated by the negative OLR anomaly, was closely tied to the cyclonic vortex (Takayabu and Nitta 1993). Near 160° E there was a transition zone where a single EOF pair contained characteristics of both TD and Rossby–gravity waves (Fig. 9b). Note how zonal wavelength in Fig. 9b expands south of the equator, and zonal velocity becomes antisymmetric in the eastern half of the grid. In the central Pacific the disturbance was primarily that of the Rossby–gravity wave (Fig. 9c), centered near the

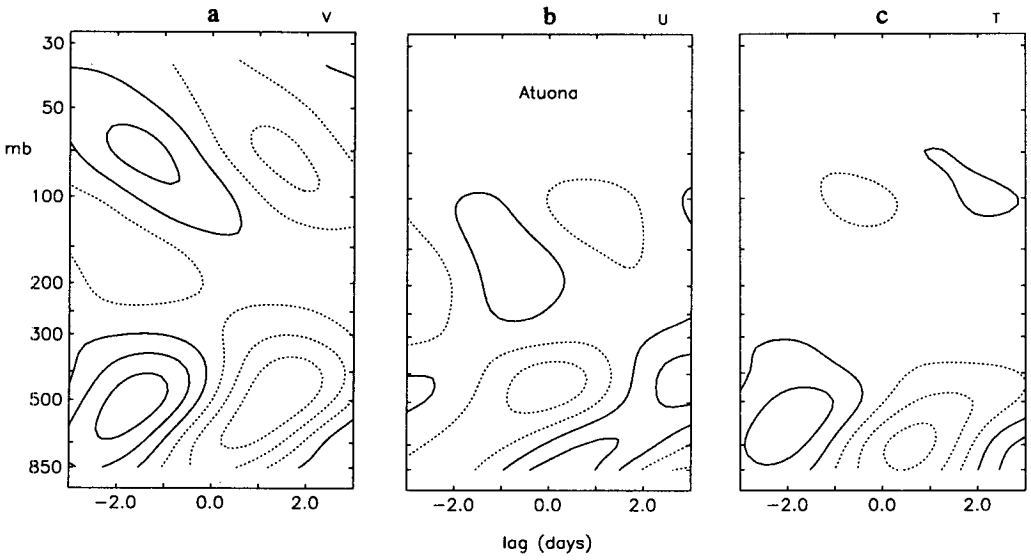

FIG. 4. As in Fig. 3 but for Atuona.

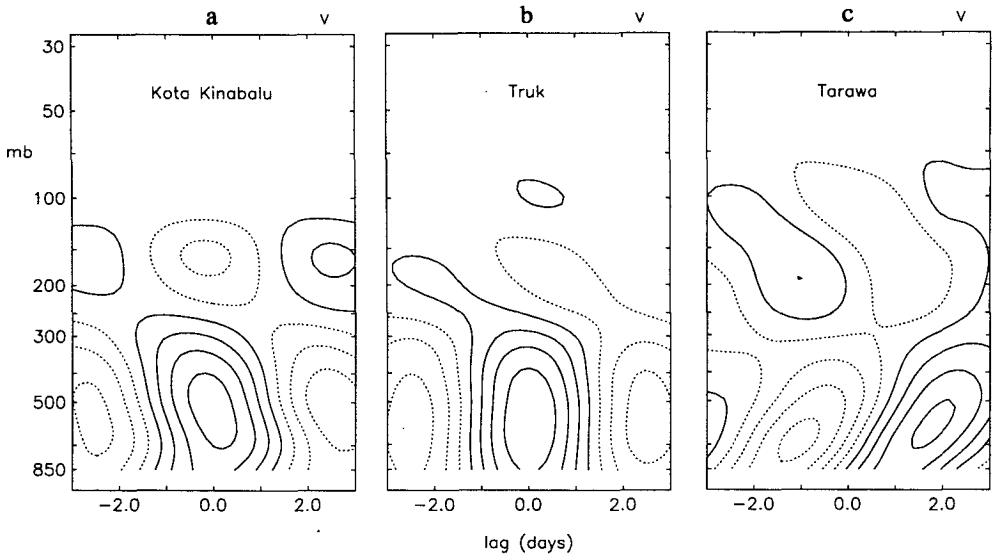

FIG. 5. As in Fig. 2 but for lower troposphere (type B) EOFs.

equator, flanked by remarkable antisymmetric OLR anomalies. In the eastern Pacific the Rossby–gravity structure persisted (Fig. 9d), accompanied by a single, weak lobe of OLR north of the equator. This observation is consistent with a tendency of the intertropical convergence zone (ITCZ) to parallel the equator on the northern side across the Pacific, while the South Pacific convergence Zone (SPCZ) slants southeastward away from the equator (Vincent 1994). East of the date line the SPCZ is too far from the equator to interact with equatorial waves. Figure 9d gives the impression, as it were, of a two-cylinder engine—representing the antisymmetric lobes of convection in Fig. 9c—running on only one cylinder. Disturbances were apparently becoming decoupled from convection in this region as the group propagated eastward. These remarks pertain to the transition of climatological structure from western to eastern Pacific, and not to any particular wave event, although examples of group propagation with structural changes can also be found in the data.

As discussed in the sequel, Rossby–gravity structures were prevalent in the 700-mb analysis throughout the central and eastern Pacific, Atlantic, and Indian Oceans. The TD disturbances were detected not only

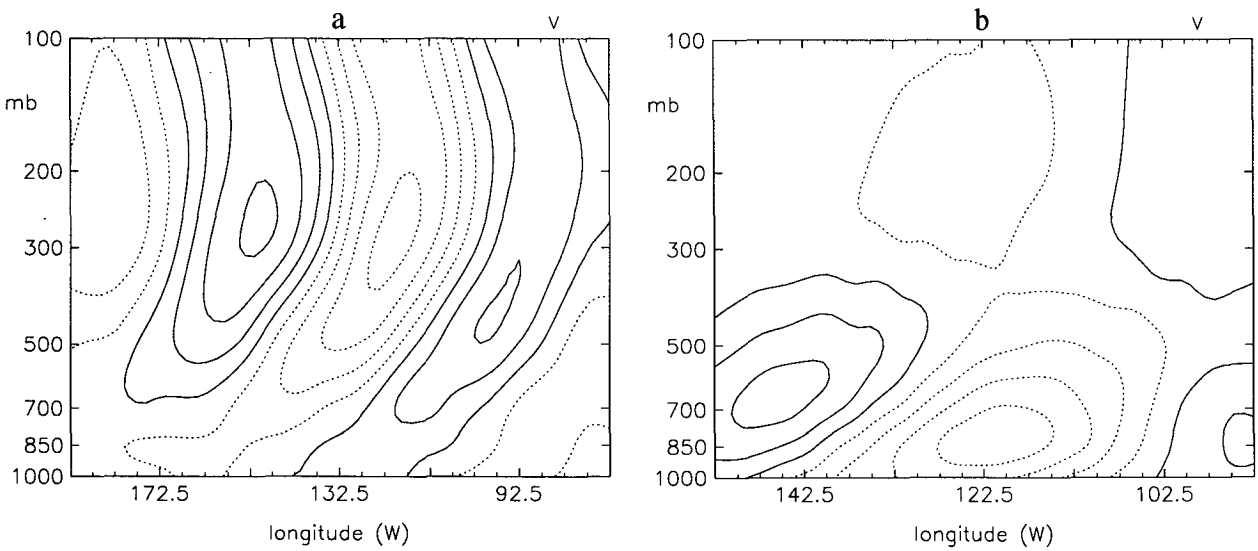

FIG. 6. Longitude–height EOFs of meridional wind from ECMWF data in east-central Pacific. (a) Upper-tropospheric mode at equator; (b) lower-tropospheric mode at 5°S.

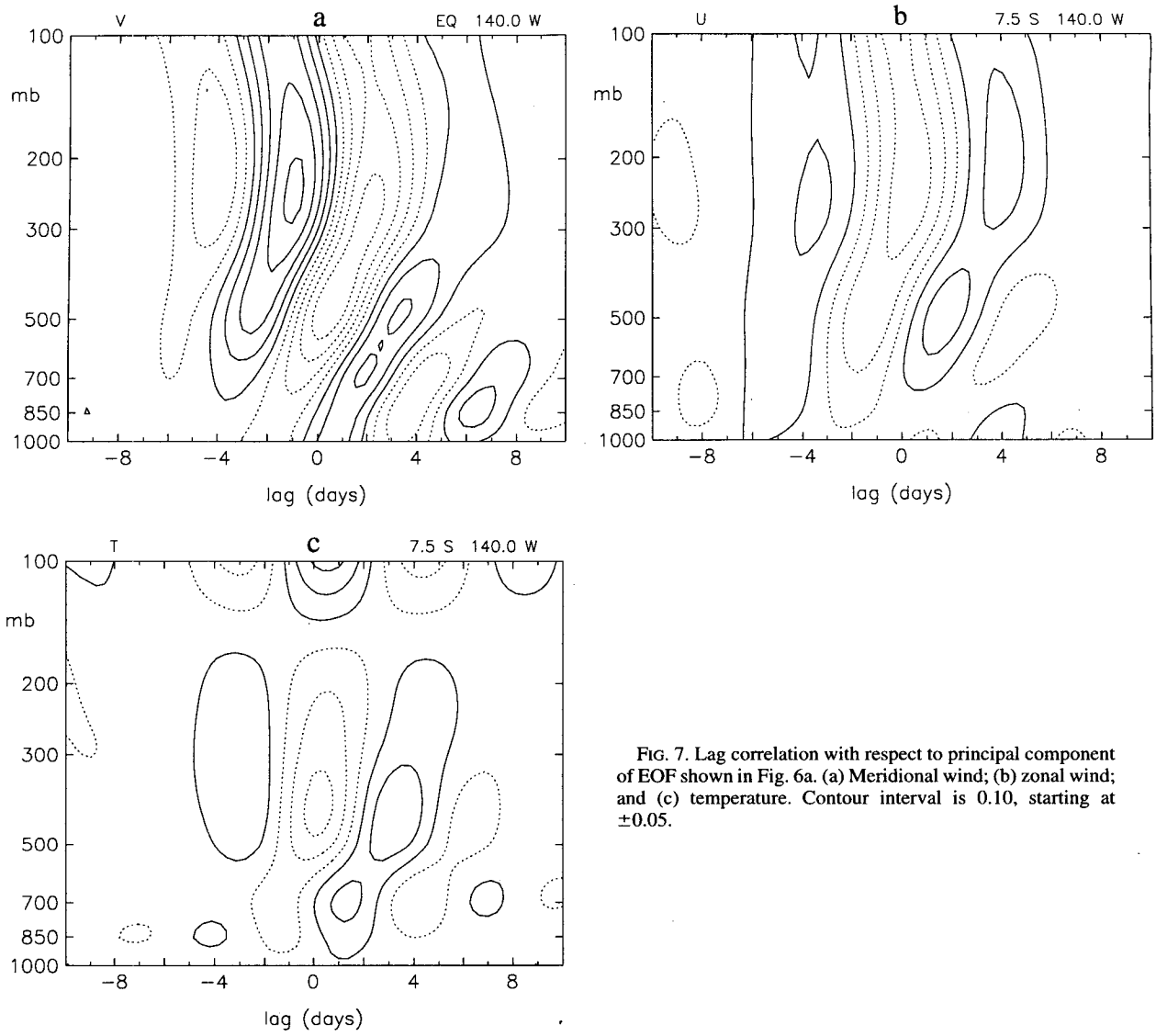

FIG. 7. Lag correlation with respect to principal component of EOF shown in Fig. 6a. (a) Meridional wind; (b) zonal wind; and (c) temperature. Contour interval is 0.10, starting at ±0.05.

in the western Pacific but (with lesser amplitude) in the Atlantic and central American sectors (Lau and Lau 1990). Weak equatorially trapped Rossby waves were found in the Atlantic (Liebmann and Hendon 1990). Subtropical latitudes were dominated by eastward moving baroclinic systems, and some evidence of meridional propagation was seen along the west coast of South America. There were noticeable variations of wave period from one region to the other, even within the same wave type, showing how the local environment is important.

4. Phase and apparent group propagation

a. Lag correlation diagrams

Several examples of lag correlation of ECMWF meridional wind with respect to principal component time series (PCs) are displayed in Figs. 10a–f. Figures 10a,b show 200–300-mb v' correlations with respect to rawinsonde type A PCs at Tarawa and Atuona. The dominant wavelength in central Pacific was 60°–80° (zonal wavenumber 4–6), in agreement with rawinsonde estimates (D93). Apparent group velocity was eastward. The situation at Atuona was rather different (Fig. 10b). The interference pattern at this location was caused by superposition of eastward moving midlatitude baroclinic systems and westward moving equatorial waves. By examining other latitudes, we found that the *same* reference series that was correlated with westward moving waves at the equator was also correlated with eastward moving waves at 22.5° S. Therefore, the type A PC at Atuona contained both types of wave. This is an obvious limitation of sin-

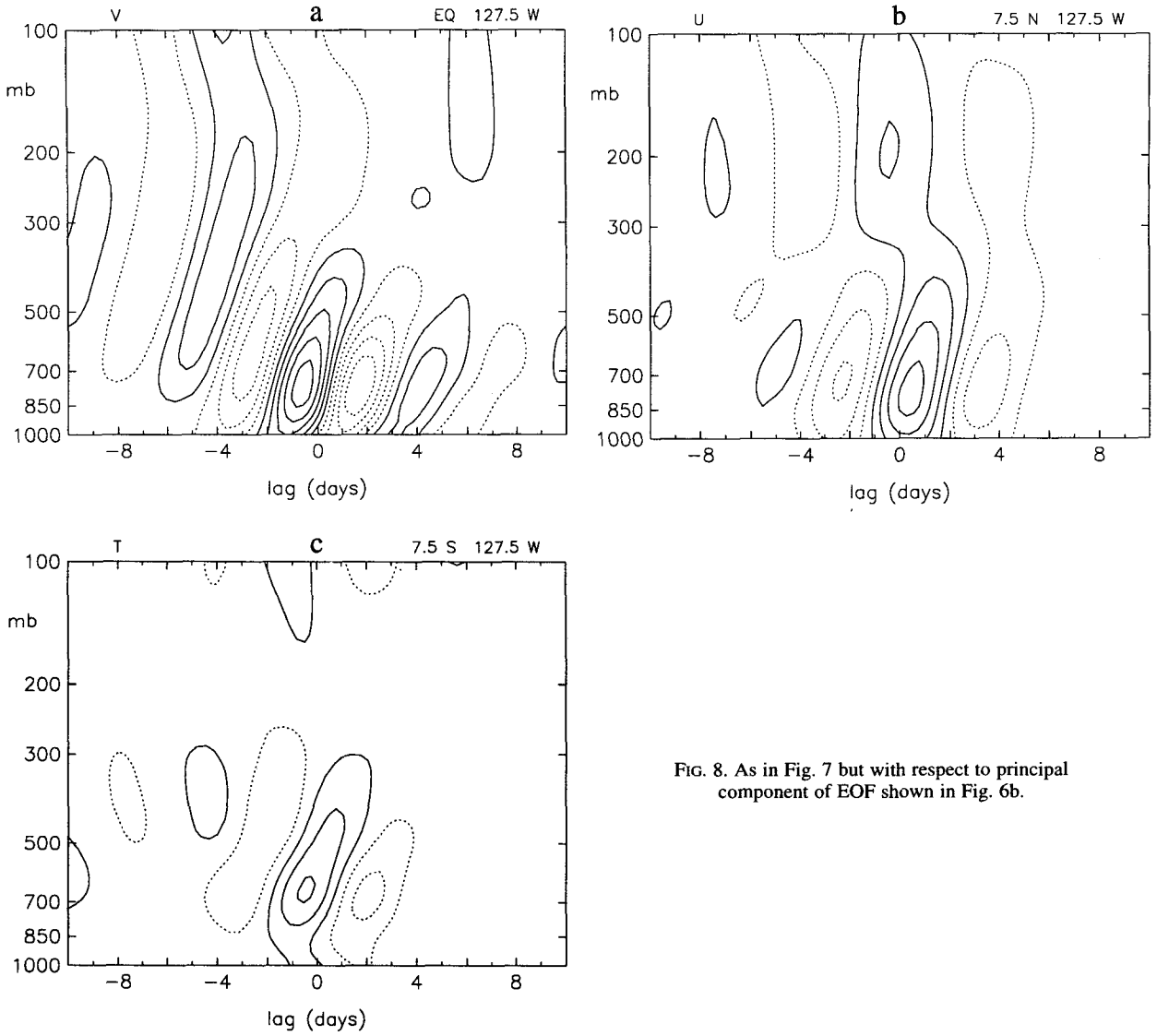

FIG. 8. As in Fig. 7 but with respect to principal component of EOF shown in Fig. 6b.

gle-station EOF analysis since nothing can be inferred about propagation direction.

Correlation with type B gave a significant response in the lower troposphere. In the far western Pacific, zonal wavelengths were shorter by a factor of two (typically 30°–40°). Figure 10c shows correlations with respect to type B at Kota Kinabalu. Zonal group velocity was poorly defined, but there was evidence of fast southward group propagation in this region, that is, a lag of 1 or 2 days between the time of maximum activity at 7.5°–15° N and its appearance near the equator (see discussion surrounding Figs. 13a,d below). Figure 10d shows the correlation with respect to type B at Majuro. In the central Pacific, the pattern mixed together short wavelengths to the west of the date line and longer wavelengths to the east—reminiscent of Nitta's (1970) rawinsonde observation. In this region type B was probably influenced by TD disturbances, as well as by lower-tropospheric equatorial waves.

The contrast between western and eastern Pacific was obvious using 700-mb ECMWF principal components as the reference series (Figs. 10e,f). Zonal wavelengths were nearly twice as long in eastern Pacific, and the periods were somewhat shorter.

Maximum correlations of ECMWF data with rawinsonde or ECMWF principal components were typically 0.50–0.70, slightly lower than gridpoint correlations mentioned in section 2 but extending over a much larger horizontal area. The percentage of spatially averaged meridional wind variance in the troposphere explained by dominant EOF pairs was typically 10%–30% (D93). Percent variance explained is an ambiguous statistic, reflecting the wave amplitude, spatial ex-

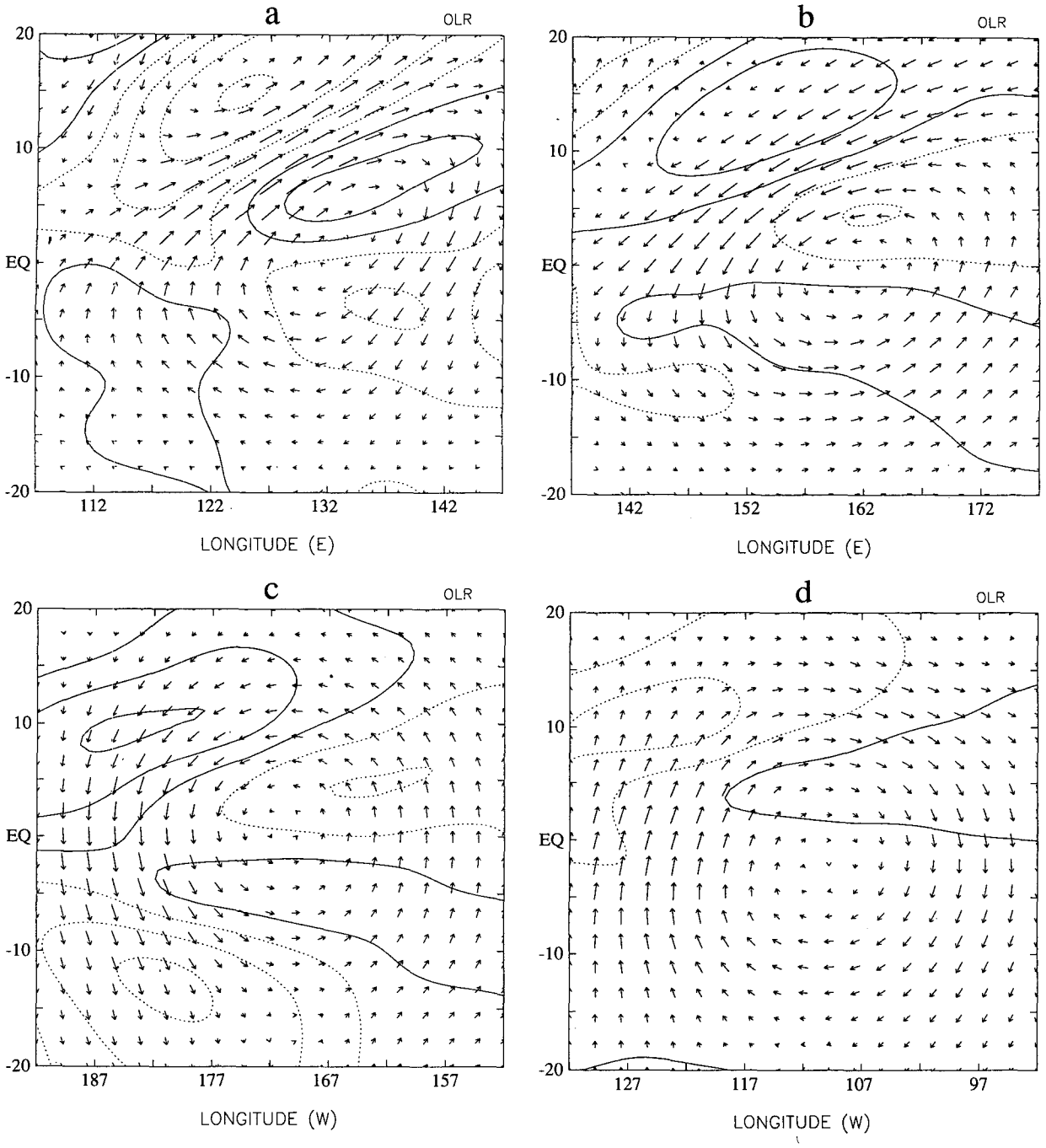

FIG. 9. Multivariate horizontal EOFs from 700-mb ECMWF and OLR data, based on the correlation matrix of horizontal wind components (vectors) and OLR (contours). (a) Far western Pacific; (b) west-central Pacific; (c) east-central Pacific; and (d) far eastern Pacific. Contour interval for OLR is 0.10, starting at ±0.05. The longest vector corresponds to a nondimensional EOF value near 0.6.

tent, and frequency of occurrence relative to other disturbances on the grid. More meaningful is the relative amplitude of waves (compared to the mean flow), which, in the lower troposphere, was generally large in the western Pacific, causing closed vortices to form, while moderate in the central and eastern Pacific, causing deflection of trade winds ~45° from the prevailing direction.

b. Wave parameters

Lag correlations were calculated with respect to ten examples of type A rawinsonde PCs (one from each

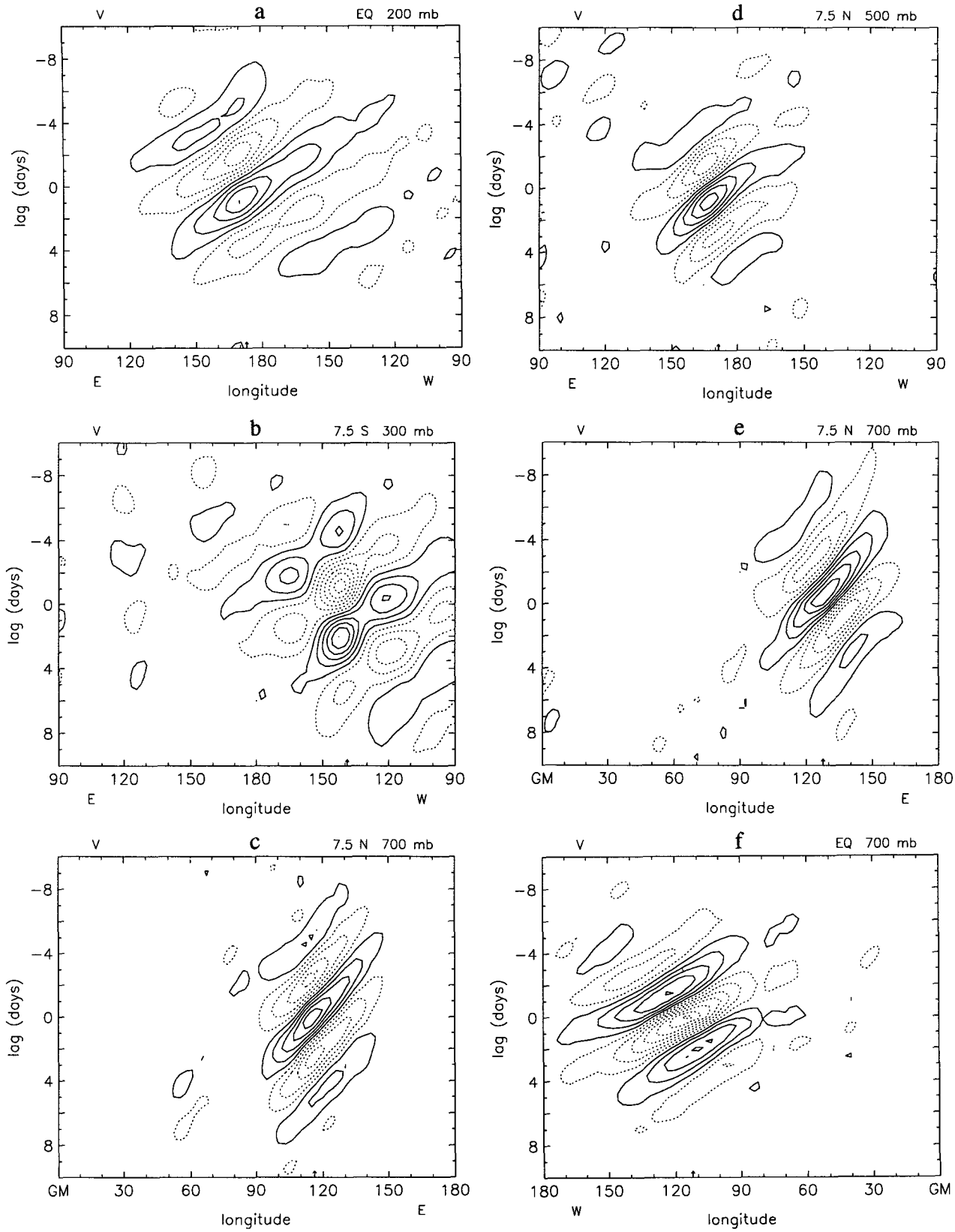

FIG. 10. Lag correlation of meridional wind with respect to principal components of rawinsonde data [(a), (b), (c), (d)] and 700-mb ECMWF and OLR data [(e), (f)]. Arrow at bottom of plot indicates station location or center of ECMWF subgrid. Data from this station (or subgrid) were used to generate the EOF and corresponding principal component time series for lag correlation analysis. Contour interval is 0.10, starting at ±0.05.

station), ten of type B, and 16 examples of 700-mb ECMWF and OLR PCs from western to eastern Pacific (at 10° intervals). Wave parameters were estimated at each pressure level (1000, 850, 700, 500, 300, 200, and 100 mb) at 15°S, 7.5°S, equator, 7.5°N, and 15°N. Zonal wavelength, phase speed, apparent group velocity, and wave period were obtained objectively by a simple routine, as illustrated in Fig. 11 using the example from Fig. 10a. Contiguous grid points exceeding a certain threshold (correlation magnitude 0.05) were grouped into clusters, a least-squares fit was obtained (for phase lines) along with a center of mass, and a second least-squares fit was drawn through the centers of mass (for apparent group velocity). Zonal wavelength and wave period were calculated between adjacent phase lines near cluster centers. Examples of zonal wavelength, phase speed, and wave period are shown in Figs. 12a–d.

In Fig. 12a, zonal wavelengths at 850 mb decreased markedly from eastern to western Pacific, as already noted. Immediately west of the date line, wavelengths appeared to decrease gradually, which is somewhat deceptive as the actual transition was more abrupt (e.g., Fig. 10d). There were longer wavelengths (with Rossby–gravity structure) in the Indian Ocean region. Wave periods at 850 mb increased noticeably from eastern to western Pacific (Fig. 12d). The contrast was most apparent in 850-mb phase speed (Fig. 12b). These values are consistent with Liebmann and Hendon (1990).

At 200 mb (Fig. 12c), phase speeds east of the date line separated into two groups (as did zonal wavelength and wave period, not shown): those associated with type A EOFs (maxima near 200 mb, denoted by an ×), and type B or 700-mb EOFs (maxima near 700 mb, denoted by a "+" or "△"). Two conclusions may be inferred from this analysis: 1) upper- and lower-tropospheric EOFs east of the date line represented distinct phenomena (D93); 2) 700-mb disturbances in this region were coherent with 200 mb v', *but not at zero lag*. Lag correlation diagrams, examples of which are shown in Fig. 13, revealed that lower-tropospheric waves were present at 200 mb in the central Pacific a few days prior to their arrival in the eastern Pacific lower troposphere (Figs. 13c,f). There was a similar delay in the central Pacific with less zonal group propagation (Figs. 13b,e). Waves at 100 mb closely followed those at 200 mb but slightly to the east (not shown). The picture obtained is that of a Rossby–gravity packet in central Pacific entering the eastern Pacific upper troposphere, diverging simultaneously upward to the stratosphere and downward to the lower troposphere. This remarkable observation from ECMWF data may explain the unusual type B correlation pattern in Atuona rawinsonde data (Fig. 4a).

In the far western Pacific, there was little evidence of zonal group propagation but an apparent equatorward propagation of the wave packet (Figs. 13a,d). Given the energetic nature of disturbances in the northwest equatorial Pacific, it would be surprising if Rossby–gravity waves were not excited as result of equatorial penetration of TD disturbances. Examples of this interaction are visible in the data (e.g., November 1981). The modest westward tilt with height of disturbances in this region suggests that if there is a significant projection onto equatorial Rossby–gravity waves, packets of these waves will initially propagate upward into the central Pacific upper troposphere and then diverge along the two ray paths noted above.

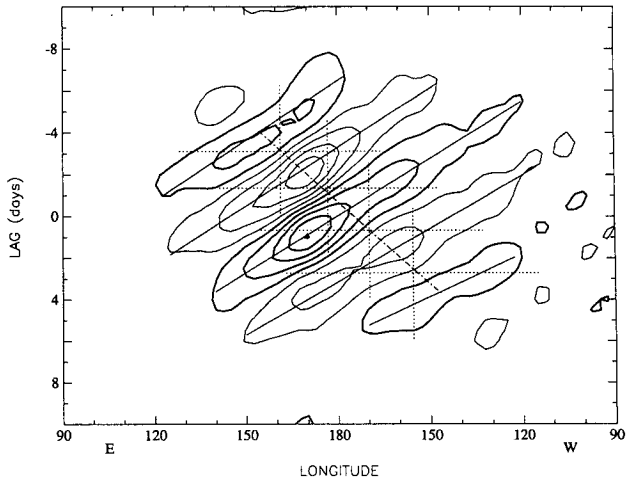

FIG. 11. Lag correlation of meridional wind as in Fig. 10a, illustrating how various wave parameters were determined.

c. *EOFs of bandpassed data*

The 700-mb multivariate EOFs were also obtained using the bandpass filters shown in Fig. 1b. As noted in section 2, the calculation was performed on a large number of subgrids of the original ECMWF grid to confirm that rotated EOFs were domain independent. The analysis established a clear distinction in each oceanic region between equatorial Rossby–gravity waves and TD disturbances with respect to frequency, zonal wavelength, cross-equatorial symmetry, and horizontal momentum flux. In the tropical Pacific lower troposphere, optimum Rossby–gravity structures were obtained from variance entirely below 5-days period, while TD disturbances were best described from variance in the 6–8-day range. By contrast, Atlantic easterly waves were primarily in the 3–4-day band; Rossby–gravity waves over the Indian Ocean had periods greater than 5 days. Zonal wavelength of TD disturbances was generally much less than that of Rossby–gravity waves. For Rossby–gravity EOFs, the center of meridional wind variance was located, on average, exactly at the equator in the Pacific and Indian Oceans and a few degrees south of the equator in the Atlantic. An advantage of EOF analysis is that we did not demand cross-equatorial symmetry a priori; nev-

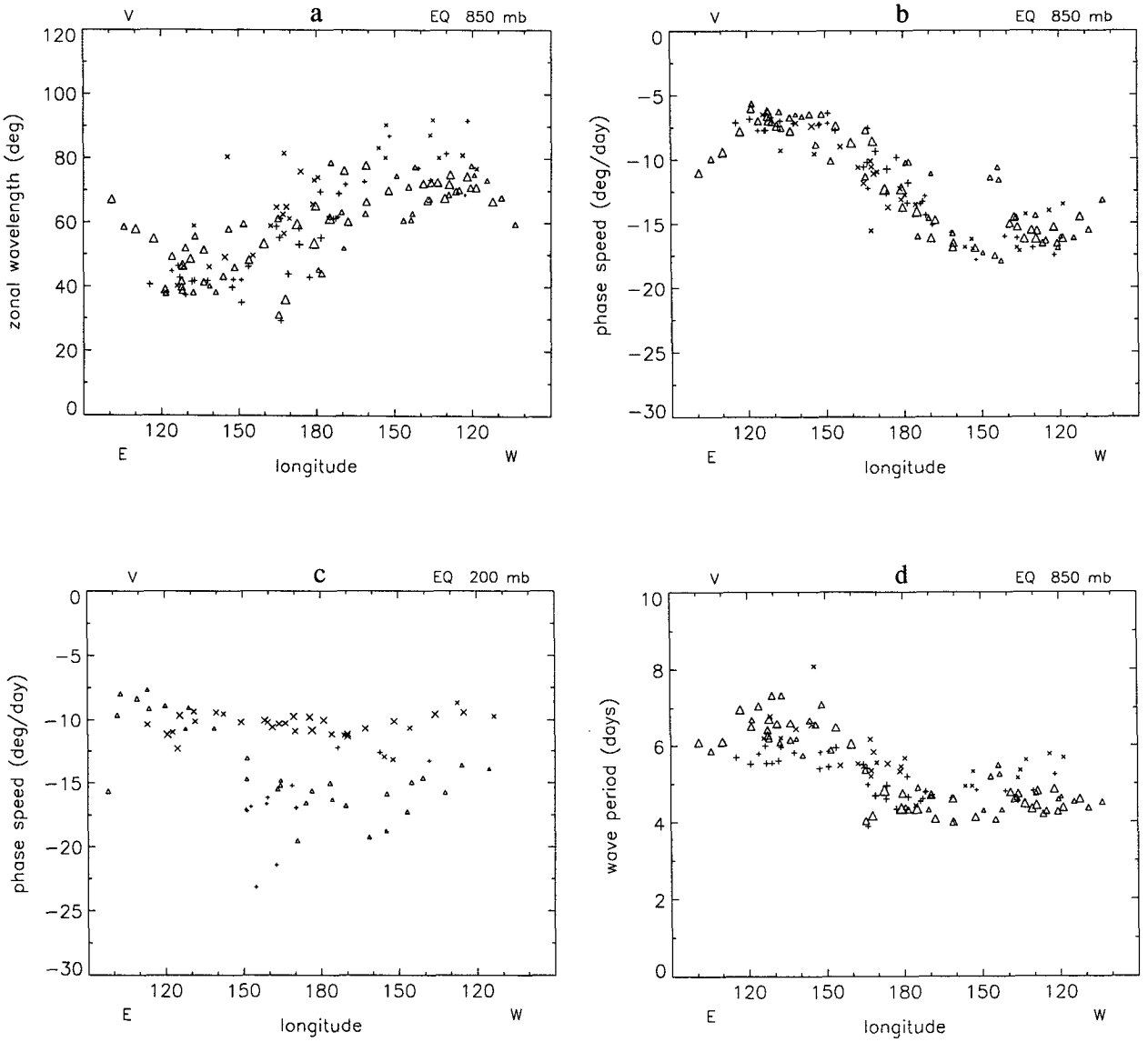

FIG. 12. Wave parameters from lag correlation analysis using principal components as reference series for rawinsonde type A (upper troposphere, ×), rawinsonde type B (lower troposphere, +), and horizontal EOFs from 700-mb ECMWF and OLR data (△). Symbol size is proportional to the average correlation within each cluster of points used to determine wave parameters (see Fig. 11). (a) Zonal wavelength at equator, 850 mb; (b) phase speed at equator, 850 mb; (c) phase speed at equator, 200 mb; and (d) wave period at equator, 850 mb.

ertheless, the expected symmetry was obtained (more or less) at all longitudes. Rossby–gravity EOFs, on average, had a negligible horizontal momentum flux correlation ($\overline{u'v'} \approx 0$). The TD disturbances had a large positive correlation—much larger, in fact, than midlatitude baroclinic waves in the same EOF calculation.

Vector plots of (u', v') lag correlation were similar to those illustrated by Liebmann and Hendon (1990), Hendon and Liebmann (1991), and Takayabu and Nitta (1993) in the western and central Pacific, so there is no need to show them again here. In the eastern Pacific, the Rossby–gravity structure was like that of the central Pacific, with weak coupling to OLR north of the equator.

5. Seasonal and interannual variations

Time series of quadrature power from rawinsonde type B EOFs and 700-mb ECMWF and OLR EOFs are shown in Figs. 14a,b, respectively. The calculation of $Q(\chi_1, \chi_2)$ between coherent principal components χ_n was described in section 5 of D93. One value of Q was plotted every 32 days and was obtained within a sliding (overlapping) window of length 128 days.

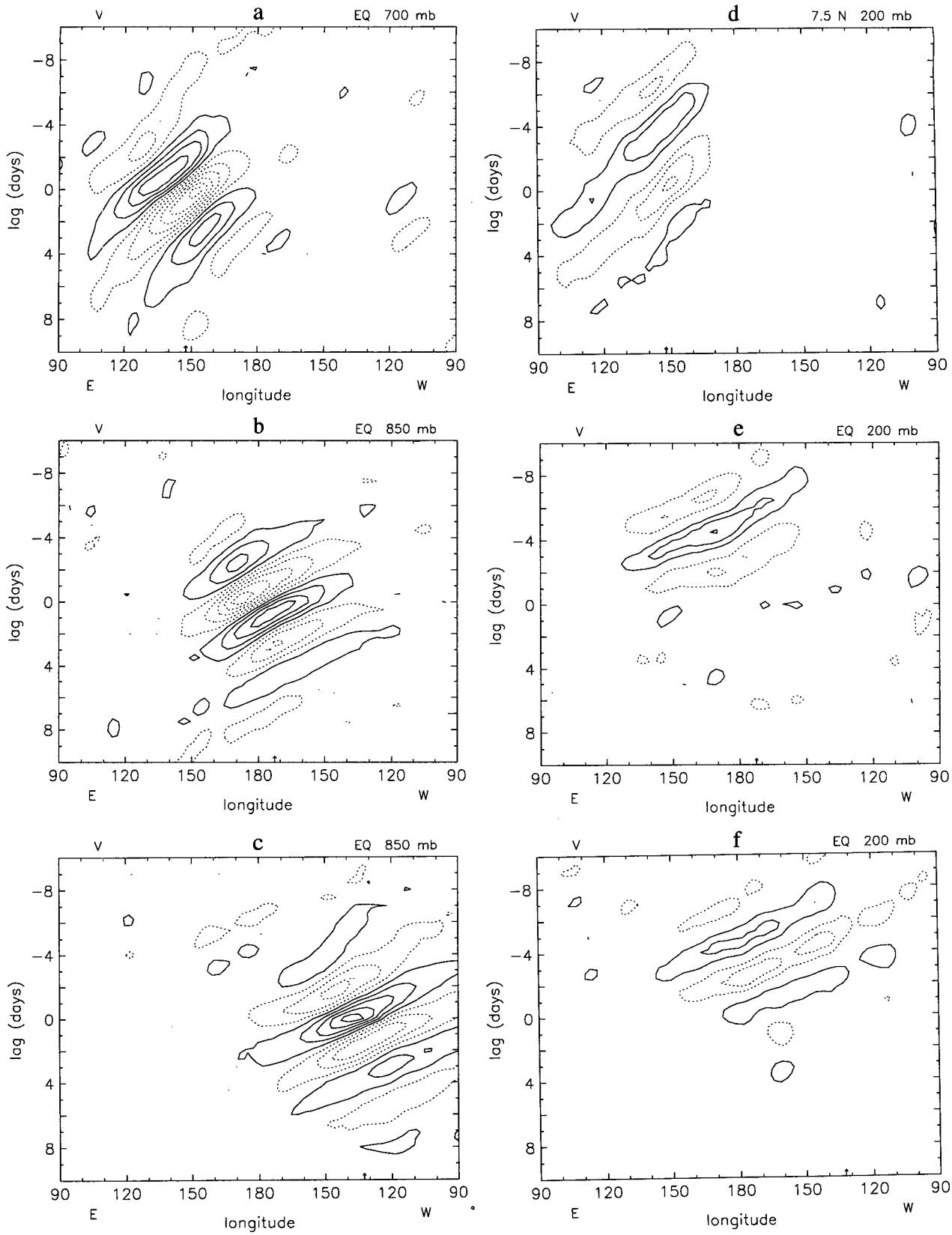

FIG. 13. Lag correlation of meridional wind as in Fig. 10, comparing lower troposphere [(a), (b), (c)] and upper troposphere [(d), (e), (f)] in western [(a), (d)], central [(b), (e)], and eastern [(c), (f)] Pacific. Reference series were obtained from horizontal EOFs of 700-mb ECMWF and OLR data; arrow at bottom of plot indicates the center of ECMWF subgrid used to generate the EOF and corresponding principal component time series. Contour interval is 0.10 in (a), (b), (c), 0.05 in (d), (e), and (f), starting at ±0.05.

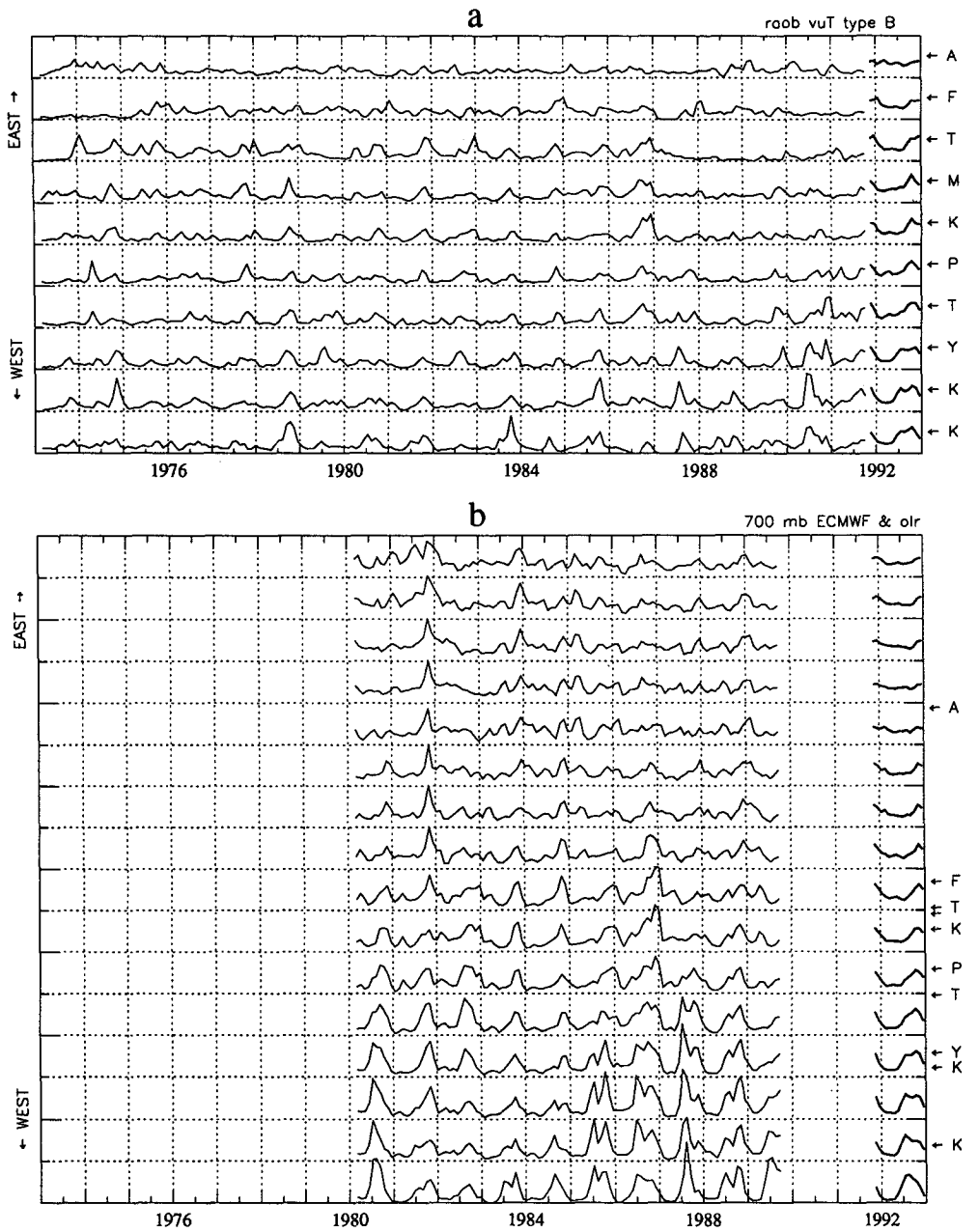

FIG. 14. Time series of quadrature power determined from (a) rawinsonde and (b) 700-mb ECMWF and OLR principal components. Average seasonal cycle is shown at far right (heavy lines). In (a), stations are displayed from western Pacific (bottom) to eastern Pacific (top) as listed in Table 1 of D93. In (b), ECMWF subgrids are displayed from western Pacific (bottom) to eastern Pacific (top) at 10° intervals, beginning at 107.5° E. Station locations are indicated by arrows on the right of (b) for comparison to (a). The date line is near Funafuti (F, 179.2° E).

The average seasonal cycle is also shown (heavy lines). For clarity, the rawinsonde seasonal cycle was magnified by a factor of two, and 1992 was omitted. Although seasonal variations in either dataset were by no means constant from year to year, it is apparent that dominant waves in the lower troposphere maximized in Northern Hemisphere (NH) summer, autumn, and winter in the western, central, and eastern Pacific, respectively. There was excellent agreement between the two datasets in this respect.

To summarize what has been suggested by earlier authors, the summer maximum in western Pacific is consistent with the time of overall warmest SST, while the autumn maximum in central Pacific reflects the ap-

pearance of twin SST maxima straddling the equator (Hendon and Liebmann 1991). The TD disturbances are strongly coupled to convection (Takayabu and Nitta 1993) but do not require a particular SST pattern. Rossby–gravity waves in the central Pacific are more loosely coupled and apparently prefer off-equatorial SST maxima (Hendon and Liebmann 1991). According to the Sadler et al. (1987) atlas, the SST contrast between the equator and ±10° latitude is strong in NH autumn (NH winter) in central (eastern) Pacific; this may explain the tendency for eastern Pacific waves to maximize a little later than central Pacific waves (Fig. 14b). We note, however, that most of the eastern Pacific activity could be traced back to the central Pacific, in accord with the apparent group propagation discussed in section 4. Thus, in a climatological sense, in situ excitation of convectively coupled Rossby–gravity waves in the eastern Pacific is unlikely when compared to the central Pacific.

Interannual variations are also apparent in Fig. 14. While there was modest agreement between the two datasets during large events (e.g., 1981 and 1986 in central Pacific, 1985 in western Pacific), the rawinsonde series were noisier, and peak to peak climatological variation were smaller, than the ECMWF/OLR series. This is to be expected since the rawinsonde value is a point measurement (as opposed to a spatial PC representing many grid points) and some spatial–temporal smoothing is inherent in the ECMWF analysis scheme.

Takayabu and Nitta (1993) suggested that ENSO modulates the lower-tropospheric waves so that equatorial waves are preferred (relative to TD disturbances) in years of relatively cold equatorial SST, and vice versa, even within the same geographical region. Although there is evidence of interannual variation in Fig. 14, it would be better to document this variability using an *evolutive principal component analysis* in which EOFs change slowly in time (D93) instead of remaining fixed to the climatological structures discussed here.

6. Conclusions

Twenty years of rawinsonde data (1973–1992) were examined in conjunction with ECMWF analyses and outgoing longwave radiation (OLR) in 1980–1989 to determine the horizontal structure, propagation, and convective coupling of 3–6-day meridional wind oscillations over the tropical Pacific. Wave properties from ECMWF data were consistent with what could be determined from the sparse rawinsonde network alone. There were significant correlations between the two datasets, using individual station observations or rawinsonde principal components as reference series; the latter gave useful results over a much wider horizontal area. Zonal wavelengths, phase speeds, and wave periods were determined objectively and agreed with previous estimates.

Gridded analyses allowed a clearer distinction between equatorially trapped Rossby–gravity waves and off-equatorial TD disturbances so that the contrasting properties of these waves, including their seasonal and interannual variation, could be studied in better detail. Zonal wavelengths of Rossby–gravity waves east of the date line in the lower troposphere were nearly twice that of TD disturbances in the far western Pacific, and westward phase speeds were larger by a factor of 3. Unlike TD disturbances in other sectors, the western Pacific waves had a relatively long period (6–8 days).

Significant correlations with OLR were found, increasing in magnitude from eastern to western Pacific. In the western Pacific, convection was tightly coupled to the cyclonic vortex of TD disturbances. For 700-mb Rossby–gravity waves in the central Pacific, the convection, by contrast, displayed a remarkable antisymmetric pattern with respect to the equator, consistent with low-level convergence. There was a transition zone in west-central Pacific where disturbances displayed characteristics of both. In the eastern Pacific, only the northern half of the antisymmetric OLR pattern survived and was somewhat weaker. This indicates that, on average, the lower-tropospheric waves were either too weak to organize convection in the southeast equatorial Pacific, or convection was too difficult to establish here due to unfavorable SST.

The apparent group propagation of disturbances was equatorward in the western Pacific, eastward across the central and eastern Pacific, and upward–downward out of the 150–300-mb layer. Vertical propagation was evident mainly at higher frequencies, implying that only a fraction of the kinetic energy associated with Rossby–gravity waves in the upper troposphere was involved either in convective coupling to the lower troposphere or vertical momentum transport to the lower stratosphere. A key result is that even though Rossby–gravity structures dominated the 150–300 layer throughout much of the tropics, their average characteristics (zonal wavelength, phase speed, and wave period) were sufficiently different from faster RGW in the lower troposphere and lower stratosphere so that two or three distinct EOF pairs were required to describe them (D93). Evidently a large component of meridional wind variance near 200 mb—much of it associated with Rossby–gravity waves and following a moist RGW dispersion relation (Randel 1992; Magaña and Yanai 1994)—tended to overwhelm the smaller, faster component responsible for convective coupling and vertical momentum transport. Nevertheless, we found significant correlation to 200 mb a few days *prior* to the arrival of waves in the lower troposphere and lower stratosphere. The vertical group velocity of Rossby–gravity waves is sensitive to intrinsic frequency, which may explain the trapping of lower-frequency waves.

Although our results establish a role for convectively coupled Rossby–gravity waves in the stratosphere, it is doubtful that all stratospheric Rossby–gravity waves are necessarily the result of convection since the B pattern explained only a fraction of stratospheric RGW and their seasonal variations were distinct (D93). Vertical radiation across the tropopause is expected regardless of convective coupling, leaving a role for laterally forced waves in the momentum balance of the lower stratosphere. Further investigation of this matter is desirable but outside the scope of this paper.

It was suggested that in addition to convective and lateral forcings, Rossby–gravity waves could be excited by energetic TD disturbances in the western Pacific. Rossby–gravity packets occasionally emerged eastward from a large TD event in the western Pacific. Although it is expected that individual RGW phases may act to "seed" TD disturbances since the phase propagation is westward (Takayabu and Nitta 1993), the direction of cause and effect is eastward according to linear theory. The observed group propagation was in fact eastward, but we caution that this is an apparent group velocity that, in general, must account for the role of saturation, dissipation, and (possibly) the motion of midlatitude sources.

Acknowledgments. The authors thank Harry Hendon for supplying OLR data in a convenient format. This research was supported by the National Aeronautics and Space Administration, Contracts NASW-4508 and NASW-4844, and by the National Science Foundation, Grant ATM-9123797.

REFERENCES

Chang, C.-P., and C. R. Miller III, 1977: Comparison of easterly waves in the tropical Pacific during two contrasting periods of sea surface temperature anomalies. *J. Atmos. Sci.*, **34,** 615–628.

Dunkerton, T. J., 1991: Intensity variation and coherence of 3–6 day equatorial waves. *Geophys. Res. Lett.*, **18,** 1469–1472.

——, 1993: Observation of 3–6 day meridional wind oscillations over the tropical Pacific, 1973–1992: Vertical structure and interannual variability. *J. Atmos. Sci.*, **50,** 3292–3307.

Ghil, M., and K. Mo, 1991: Intraseasonal oscillations in the global atmosphere. Part I: Northern Hemisphere and Tropics. *J. Atmos. Sci.*, **48,** 752–779.

Hack, J. J., W. H. Schubert, D. E. Stevens, and H.-C. Kuo, 1989: Response of the Hadley circulation to convective forcing in the ITCZ. *J. Atmos. Sci.*, **46,** 2957–2973.

Hendon, H. H., and B. Liebmann, 1991: The structure and annual variation of antisymmetric fluctuations of tropical convection and their association with Rossby–gravity waves. *J. Atmos. Sci.*, **48,** 2127–2140.

Hess, P. G., D. S. Battisti, and P. J. Rasch, 1993: Maintenance of the intertropical convergence zones and the large-scale tropical circulation on a water-covered earth. *J. Atmos. Sci.*, **50,** 691–713.

Lau, K.-H., and N.-C. Lau, 1990: Observed structure and propagation characteristics of tropical summertime synoptic scale disturbances. *Mon. Wea. Rev.*, **118,** 1888–1913.

——, and ——, 1992: The energetics and propagation dynamics of tropical summertime synoptic-scale disturbances. *Mon. Wea. Rev.*, **120,** 2523–2539.

Liebmann, B., and H. H. Hendon, 1990: Synoptic-scale disturbances near the equator. *J. Atmos. Sci.*, **47,** 1463–1479.

Magaña, V., and M. Yanai, 1995: Mixed Rossby–gravity waves triggered by lateral forcing. *J. Atmos. Sci.*, **52,** 1473–1486.

Mapes, B. E., and R. A. Houze Jr., 1993: Cloud clusters and superclusters over the oceanic warm pool. *Mon. Wea. Rev.*, **121,** 1398–1415.

Maruyama, T., 1991: Annual variations and QBO-synchronized variations of the equatorial wave intensity in the lower stratosphere at Singapore during 1961–1989. *J. Meteor. Soc. Japan,* **69,** 219–232.

Nakazawa, T., 1988: Tropical super clusters within intraseasonal variations over the western Pacific. *J. Meteor. Soc. Japan,* **66,** 823–839.

Nitta, T., 1970: Statistical study of tropospheric wave disturbances in the tropical Pacific region. *J. Meteor. Soc. Japan,* **48,** 47–59.

——, and Y. Takayabu, 1985: Global analysis of the lower tropospheric disturbances in the tropics during the northern summer of the FGGE year. Part II: Regional characteristics of the disturbances. *Pure and Appl. Geophys.*, **123,** 272–292.

——, Y. Nakagomi, Y. Suzuki, N. Hasegawa, and A. Kadokura, 1985: Global analysis of the lower tropospheric disturbances in the tropics during the northern summer of the FGGE year. Part I: Global features of the disturbances. *J. Meteor. Soc. Japan,* **63,** 1–19.

Randel, W. J., 1992: Upper tropospheric equatorial waves in ECMWF analyses. *Quart. J. Roy. Meteor. Soc.*, **118,** 365–394.

Sadler, J. C., M. A. Lander, A. M. Hori, and L. K. Oda, 1987: Tropical Marine Climatic Atlas, Vol. II: Pacific Ocean. Department of Meteorology, University of Hawaii Rep. UHMET 87-02.

Takayabu, Y. N., and T. Nitta, 1993: 3–5 day period disturbances coupled with convection over the tropical Pacific ocean. *J. Meteor. Soc. Japan,* **71,** 221–246.

Vincent, D. G., 1994: The South Pacific Convergence Zone (SPCZ): A review. *Mon. Wea. Rev.*, **122,** 1949–1970.

Wallace, J. M., 1971: Spectral studies of tropospheric wave disturbances in the tropical western Pacific. *Rev. Geophys. Space Phys.*, **9,** 557–612.

Yanai, M., 1975: Tropical meteorology. *Rev. Geophys. Space Phys.*, **13,** 685–710, 800–808.

——, and T. Maruyama, 1966: Stratospheric wave disturbances propagating over the equatorial Pacific. *J. Meteor. Soc. Japan,* **44,** 291–294.

——, and Y. Hayashi, 1969: Large-scale equatorial waves penetrating from the upper troposphere into the lower stratosphere. *J. Meteor. Soc. Japan,* **47,** 167–182.

——, and M.-M. Lu, 1983: Equatorially trapped waves at the 200-mb level and their association with meridional convergence of wave energy flux. *J. Atmos. Sci.*, **40,** 2785–2803.

——, T. Maruyama, T. Nitta, and Y. Hayashi, 1968: Power spectra of large-scale disturbances over the tropical Pacific. *J. Meteor. Soc. Japan,* **46,** 308–323.

Zangvil, A., and M. Yanai, 1980: Upper tropospheric waves in the tropics, Part I: Dynamical analysis in the wavenumber-frequency domain. *J. Atmos. Sci.*, **37,** 283–298.

——, and ——, 1981: Upper tropospheric waves in the tropics, Part II: Association with clouds in the wavenumber-frequency domain. *J. Atmos. Sci.*, **38,** 939–953.